Puromycin aminonucleoside induces oxidant-dependent DNA damage in podocytes *in vitro* and *in vivo*

CB Marshall[1], JW Pippin[1], RD Krofft[1] and SJ Shankland[1]

[1]*Division of Nephrology, University of Washington, Seattle, Washington, USA*

A decline in podocyte number correlates with progression to glomerulosclerosis. A mechanism underlying reduced podocyte number is the podocyte's relative inability to proliferate in response to injury. Injury by the podocyte toxin puromycin aminonucleoside (PA) is mediated via reactive oxygen species (ROS). The precise role of ROS in the pathogenesis of PA-induced glomerulosclerosis remains to be determined. We sought to examine whether PA-induced ROS caused podocyte DNA damage, possibly accounting for the podocyte's inability to proliferate in response to PA. *In vitro*, podocytes were exposed to PA, with or without the radical scavenger 1,3-dimethyl-2-thiourea (DMTU). *In vivo*, male Sprague–Dawley rats were divided into experimental groups ($n = 6$/group/time point): PA, PA with DMTU, and control, killed at days 1.5, 3, or 7. DNA damage was measured by DNA precipitation, apurinic/apyrimidinic site, Comet, and 8-hydroxydeoxyguanosine assays. Cell cycle checkpoint protein upregulation (by immunostaining and Western blotting), histopathology, and biochemical parameters were examined. DNA damage was increased in cultured podocytes that received PA, but not PA with DMTU. PA exposure activated specific cell cycle checkpoint proteins, with attenuation by DMTU. DNA repair enzymes were activated, providing evidence for attempted DNA repair. The PA-treated animals developed worse proteinuria and histopathologic disease and exhibited more DNA damage than the DMTU pretreated group. No significant apoptosis was detected by terminal deoxynucleotidyl transferase-mediated dUTP nick end-labeling staining. A mechanism underlying the lack of podocyte proliferation following PA-induced injury *in vitro* and *in vivo* may be ROS-mediated DNA damage, with upregulation of specific cell cycle checkpoints leading to cell cycle arrest.

Kidney International (2006) **70,** 1962–1973. doi:10.1038/sj.ki.5001965; published online 11 October 2006

Correspondence: *SJ Shankland, Division of Nephrology, University of Washington, 1959 NE Pacific Street, Box 356521, Seattle, Washington 98195, USA. E-mail: stuartjs@u.washington.edu*

Received 19 October 2005; revised 17 August 2006; accepted 18 August 2006; published online 11 October 2006

KEYWORDS: podocyte; DNA damage; puromycin aminonucleoside nephropathy; reactive oxygen species; proliferation; glomerulosclerosis

The glomerular visceral epithelial cell, or podocyte, is a highly specialized and terminally differentiated cell that forms a critical part of the glomerular filtration barrier and functions to prevent urinary protein leakage, maintain glomerular capillary loop integrity, oppose intracapillary hydrostatic pressure, and synthesize the glomerular basement membrane.[1] Common to many human kidney diseases and experimental animal models is a strong association between podocyte injury and glomerulosclerosis. Studies have demonstrated that a decline in podocyte number strongly correlates with, and likely underlies, progression to glomerulosclerosis.[2–6] Two important mechanisms for podocyte depletion following injury are apoptosis and detachment. Podocyte loss leads to areas of denuded basement membrane, culminating in proteinuria, the development of focal glomerulosclerosis, and progressive deterioration in kidney function.

Owing to their highly differentiated state, mature podocytes readily do not proliferate *in vivo*. Therefore, the apparent lack of proliferation in response to injury contributes to reduced podocyte number.[2] At the cell cycle level, reduced proliferation is a consequence of either an abnormality in DNA synthesis, secondary to G_1/S checkpoint arrest, or reduced mitosis, secondary to G_2/M checkpoint arrest. DNA damage triggers activation of cell cycle checkpoints, molecular pathways that monitor passage through the cell cycle and generate pauses in cell cycle progression when DNA damage is present. Thus, DNA damage leads to cell cycle arrest, permitting the cell sufficient time for DNA repair or other cell fate decisions, including apoptosis or entry into a permanent senescence-like state, thereby limiting proliferation.[7] Cell cycle arrest following DNA damage is mediated, in part, by tumor suppressor p53 and cyclin-dependent kinase inhibitor $p21^{WAF1/CIP1}$. It is unknown whether the presence of DNA damage, with subsequent cell cycle arrest, accounts for the podocyte's limited proliferation in non-immune-mediated podocyte injury, namely puromycin aminonucleoside nephropathy (PAN).

Puromycin aminonucleoside (PA), a podocyte toxin used to induce experimental minimal change disease progressing to focal segmental glomerulosclerosis in rats, leads to podocyte foot process effacement, and massive proteinuria within 7–10 days. *In vivo* studies have supported that, acutely, PA-induced glomerular injury is mediated via overproduction of reactive oxygen species (ROS),[8–14] which then may interact with biomolecules, leading to modification and potentially deleterious cellular consequences.[15] This study was designed to examine whether DNA damage occurs in PAN, if DNA damage accounts for the inability of podocytes to proliferate in response to the toxin PA, and which cell cycle regulatory proteins may underlie this response.

RESULTS

DNA damage in cultured podocytes exposed to PA, oxidant-dependent

To determine whether PA induced DNA damage *in vitro*, growth-restricted podocytes were exposed to PA, and DNA damage was measured by three methods. DNA precipitation assay results are shown in Figure 1. As there is a basal level of oxidative DNA damage owing to non-pathogenic metabolic processes in healthy aerobic organisms,[15,16] the amount of single-stranded DNA (ssDNA) present in control cells at the earliest time point was considered the reference. This basal level of ssDNA was subtracted from subsequent values for all conditions and time points. At 6 h, there was a significant difference in the percent ssDNA between podocytes exposed to PA versus control conditions (control = 22.43%, PA = 37.08%; $P < 0.05$). There was no significant difference between these two groups at 2 and 24 h. Podocytes exposed to PA + 1,3-dimethyl-2-thiourea (DMTU) exhibited a lower percent ssDNA at 6 and 24 h than cells exposed to PA alone, with values falling below the basal level observed in control cells.

To confirm that PA mediates DNA damage, the results of the AP (apurinic/apyrimidinic or abasic) site assay are shown in Figure 2. With PA exposure, there were an increased number of abasic sites in DNA at 6 and 18 h (values per 100 000 base pairs: 6 h: control = 0.102, PA = 14.649, $P < 0.05$; 18 h: control = 1.396, PA = 2.689, $P < 0.05$). In podocytes exposed to PA + DMTU, DNA damage was lessened, with no significant increase in abasic sites when compared to controls (6 h: 0.078, 18 h: 1.441). Cells exposed to H_2O_2, the positive control for oxidant-mediated DNA damage, exhibited levels of abasic sites intermediate between control and PA groups (data not shown).

As further corroboration that PA mediates DNA damage in podocytes, the results of the Comet assay are shown in Figure 3. Following exposure to experimental conditions, podocytes underwent harvesting, immobilization in agarose, gentle lysis, and alkaline electrophoresis. With PA exposure, there was an increase in cells exhibiting long 'comet tails', when compared to control group (Figure 3a and c), at 2 and 6 h (values per 200 cells: 2 h: control = 0.8, PA = 7, $P < 0.05$; 6 h: control = 1.2, PA = 22, $P < 0.05$) (Figure 3d). In podocytes exposed to PA + DMTU, DNA damage was lessened, with a decrease in long 'comet tails' when compared to PA-exposed cells (2 h: PA + DMTU = 1.8, $P < 0.05$; 6 h: PA + DMTU = 7, $P < 0.05$) (Figure 3b).

The results from the DNA precipitation, AP site, and Comet assays demonstrated that PA caused DNA damage in cultured podocytes. This DNA damage was attenuated by pre-exposure to DMTU, providing support that PA mediated oxidative DNA damage.

Cell cycle checkpoint activation in cultured podocytes exposed to PA, oxidant-dependent

In contrast to other glomerular cells, podocytes typically do not proliferate following injury. To test the hypothesis that following PA-mediated oxidative DNA damage, cell cycle

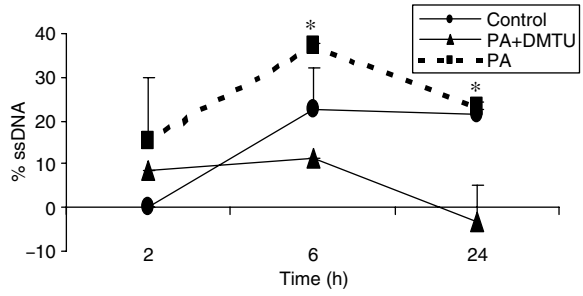

Figure 1 | PA-induced DNA damage in cultured podocytes, attenuated by pre-exposure to DMTU: DNA precipitation assay. The ssDNA was measured by the DNA precipitation assay, performed on cultured podocytes following exposure to PA 30 μg/ml at time points 2, 6, and 24 h, with or without pre-exposure to the antioxidant DMTU 10 mM. PA induced significant DNA damage at time points 6 and 24 h, an effect reduced by DMTU. As there is a basal quantity of ssDNA owing to endogenous processes, the level of ssDNA present in the control cells at the earliest time point was the reference point for all other measurements and this level of baseline ssDNA was subtracted from other values. *$P < 0.05$, for PA versus PA + DMTU.

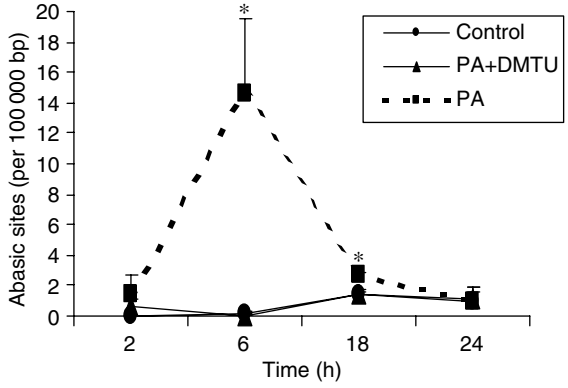

Figure 2 | PA-induced DNA damage in cultured podocytes, attenuated by pre-exposure to DMTU: AP site assay. Abasic sites were measured by the AP site assay in cultured podocytes following exposure to PA 30 μg/ml at time points 2, 6, 18, and 24 h, with or without pre-exposure to DMTU 10 mM. Following exposure to PA, at 6 and 18 h, there was a statistically significant increase in abasic sites compared with time-matched controls, an effect reduced by DMTU. *$P < 0.05$, for PA versus PA + DMTU.

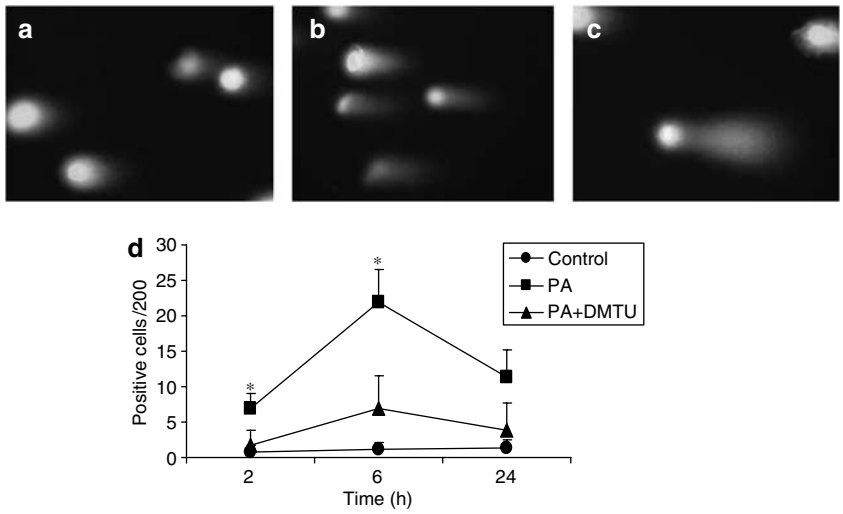

Figure 3 | PA-induced DNA damage in cultured podocytes, attenuated by pre-exposure to DMTU: Comet (single-cell gel electrophoresis) assay. Damaged DNA was measured by the Comet assay in cultured podocytes following exposure to PA 30 μg/ml at time point 2, 6, and 24 h, with or without pre-exposure to DMTU 10 mM (original magnification $\times$ 20). (**a**) Representative micrograph of fluorescent DNA stain of control cells, showing undamaged and supercoiled DNA remaining within the nuclear cell membrane. (**b**) Representative micrograph of fluorescent DNA stain of PA + DMTU-exposed cells, showing mild degree of denatured DNA fragments migrating out from cell. (**c**) Representative micrograph of fluorescent DNA stain of PA-exposed cells, showing denatured DNA fragments migrating out from cell in a long 'comet tail'. (**d**) Quantification of podocytes with long 'comet tails'. Following exposure to PA, at 2, 6, and 24 h, there was a statistically significant increase in the number of cells with long 'comet tails' compared with time-matched controls. DMTU significantly lessened PA-induced DNA damage at time points 2 and 6 h. *$P < 0.05$, for PA versus PA + DMTU.

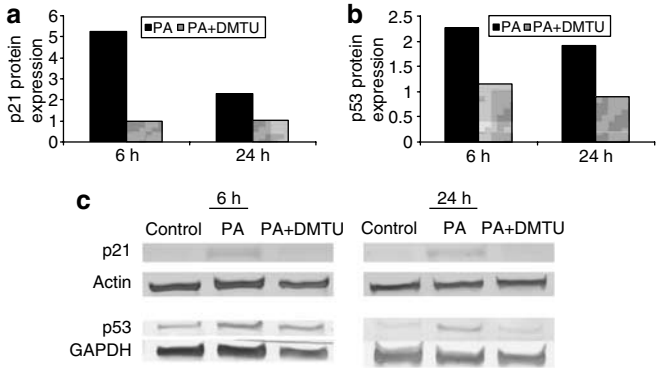

Figure 4 | Activation of cell cycle checkpoint proteins in cultured podocytes, following exposure to PA, attenuated by DMTU. (**a**) $p21^{WAF1/CIP1}$ protein expression. The protein expression of $p21^{WAF1/CIP1}$ was increased by a ratio of 5.24 and 2.28 in PA-exposed cells, compared to time-matched controls, at time points 6 and 24 h, respectively. With DMTU pre-exposure, the ratio decreased to 0.98 and 1.0, at time points 6 and 24 h, respectively. Values are averages of three separate experiments and are normalized for differences in protein loading. (**b**) p53 protein expression. The protein expression of p53 was increased by a ratio of 2.27 and 1.91 in PA-exposed cells, compared to time-matched controls, at time points 6 and 24 h, respectively. With DMTU pre-exposure, the ratio decreased to 1.16 and 0.89, at time points 6 and 24 h, respectively. Values are averages of three separate experiments and are normalized for differences in protein loading. (**c**) Western blot analysis. Representative Western blots for $p21^{WAF1/CIP1}$ and p53 are shown. Actin and glyceraldehyde-3-phosphate dehydrogenase were used as housekeeping proteins to ensure equal protein loading. The results show that $p21^{WAF1/CIP1}$ and p53 protein levels increased following exposure to PA. This was reduced by DMTU.

checkpoint proteins are activated thereby limiting proliferation, Western blotting was performed on extracts from cultured podocytes (Figure 4). At 6 and 24 h after PA exposure, protein expression was increased for $p21^{WAF1/CIP1}$ (ratio to control: 5.24 at 6 h, 2.28 at 24 h) and p53 (ratio to control: 2.27 at 6 h, 1.91 at 24 h). In podocytes pretreated with DMTU, the levels of $p21^{WAF1/CIP1}$ (ratio to control: 0.98 at 6 h, 1.02 at 24 h) and p53 (ratio to control: 1.16 at 6 h, 0.89 at 24 h) were reduced compared to the PA-only group. The expression levels of checkpoint proteins checkpoint kinase 1 (CHK-1), checkpoint kinase 2 (CHK-2), and growth arrest, DNA damage-inducible-45α were not significantly different between PA and PA + DMTU groups at 6 and 24 h (data not shown).

These results established that specific cell cycle checkpoint proteins were activated in response to PA-mediated oxidative DNA damage. Following pre-exposure to DMTU, PA did not induce the same level of cell cycle checkpoint protein activation.

DNA repair enzyme activation in cultured podocytes exposed to PA, oxidant-dependent

To determine if podocytes possessed the capacity to repair damaged DNA, specific DNA repair enzymes were evaluated. Figure 5 shows that, in addition to upregulation of cell cycle checkpoint proteins in response to PA-mediated oxidative DNA damage, there was also upregulation in DNA repair enzymes AP-endonuclease and DNA polymerase-β. By Western blotting, at 6 and 24 h, there was increased protein

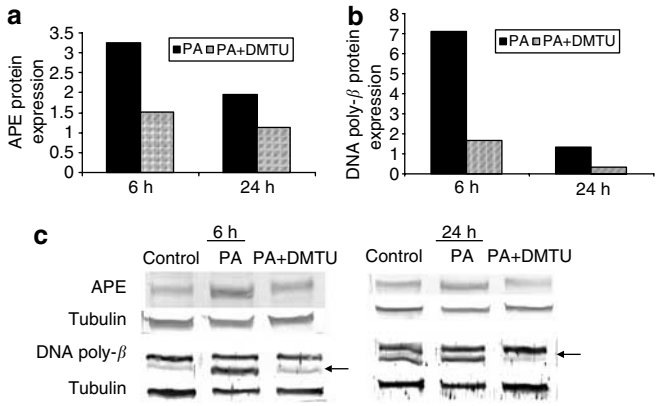

Figure 5 | Induction of DNA repair enzymes apurinic/apyrimidinic endonuclease (APE) and DNA polymerase-β (DNA poly-β) following treatment with PA, attenuated by DMTU. (**a**) APE protein expression. The protein expression of APE was increased by a ratio of 3.24 and 1.96 in PA-exposed cells, compared with time-matched controls, at time points 6 and 24 h, respectively. With DMTU pre-exposure, the ratio decreased to 1.51 and 1.13, at time points 6 and 24 h, respectively. Values are averages of three separate experiments and are normalized for differences in protein loading. (**b**) DNA poly-β protein expression. The protein expression of DNA poly-β was increased by a ratio of 7.1 and 1.34 in PA-exposed cells, compared with time-matched controls, at time points 6 and 24 h, respectively. With DMTU pre-exposure, the ratio was decreased to 1.65 and 0.33, at time points 6 and 24 h, respectively. Values are averages of three separate experiments and are normalized for differences in protein loading. (**c**) Western blot analysis. Representative Western blots for APE and DNA poly-β are shown. Tubulin was used as a housekeeping protein to ensure equal protein loading. The results show that APE and DNA poly-β protein levels increased following exposure to PA. This was reduced by DMTU. Arrows indicate band of interest.

expression of AP-endonuclease (ratio to control: 3.24 at 6 h, 1.96 at 24 h) and DNA polymerase-β (ratio to control: 7.1 at 6 h, 1.34 at 24 h) following PA exposure. Upon exposure to PA with DMTU, the levels were decreased at 6 and 24 h (AP-endonuclease ratio to control: 1.51 at 6 h, 1.13 at 24h; DNA polymerase-β ratio to control: 1.65 at 6 h, 0.33 at 24 h).

These results demonstrated that DNA repair enzymes AP-endonuclease and DNA polymerase-β were activated following PA exposure, providing indirect support that DNA damage was present and that the 'appropriate' response to injury was activated in podocytes. Decreased repair enzyme activation was seen in podocytes exposed to PA + DMTU, further supporting that DNA damage was oxidant-dependent.

Proteinuria and histopathology in PAN, oxidant-dependent

There was no significant difference in plasma blood urea nitrogen measurements in rats receiving PA versus PA + DMTU (data not shown). However, by day 7, rats receiving PA alone had significantly greater proteinuria than rats pretreated with DMTU (PA = 28.73 mg/24h; PA + DMTU = 15.85 mg/24 h; $P < 0.05$) (Figure 6a). To semiquantitatively assess the severity of glomerular injury, a glomerular sclerosis index was calculated by examining histopathologic sections stained with periodic acid-Schiff, as described previously,[17–19] using the following scale: 0 = normal glomerulus, 1 = sclerotic area ⩽25% of glomerular area, 2 = 25–50% of glomerular area, 3 = 50–75% of glomerular area, and 4 = global sclerosis. The glomerular sclerosis index was calculated by multiplying the number of glomeruli with a sclerosis score of 1 by one, 2 by two, and so on. These values were summed to obtain the final glomerular sclerosis index.

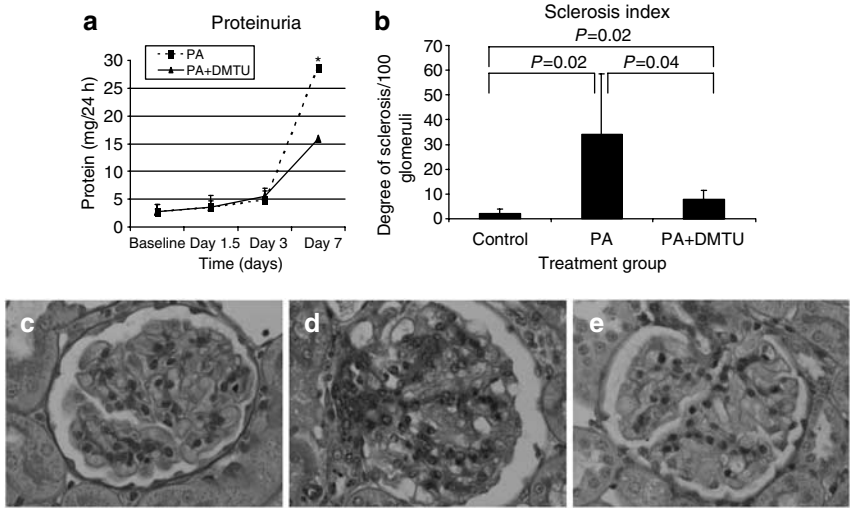

Figure 6 | Protein excretion and histopathologic changes by periodic acid-Schiff (PAS) staining following treatment with PA, with or without pre-exposure to DMTU. (**a**) Proteinuria. By day 7, rats receiving PA alone had a statistically significantly greater degree of protein excretion than rats pretreated with DMTU. *$P < 0.05$. (**b**) Sclerosis index. Tissue from rats receiving PA alone exhibited greater disease severity as semiquantitatively assessed by sclerosis index. The number of early glomerular sclerotic lesions was reduced in the PA + DMTU group ($P < 0.05$). (**c**) Histopathology (original magnification × 40). Representative micrographs of PAS staining of tissues are shown (**c** = control, **d** = PA, and **e** = PA + DMTU). Tissue from rats receiving PA alone exhibited greater disease severity than rats that received PA + DMTU.

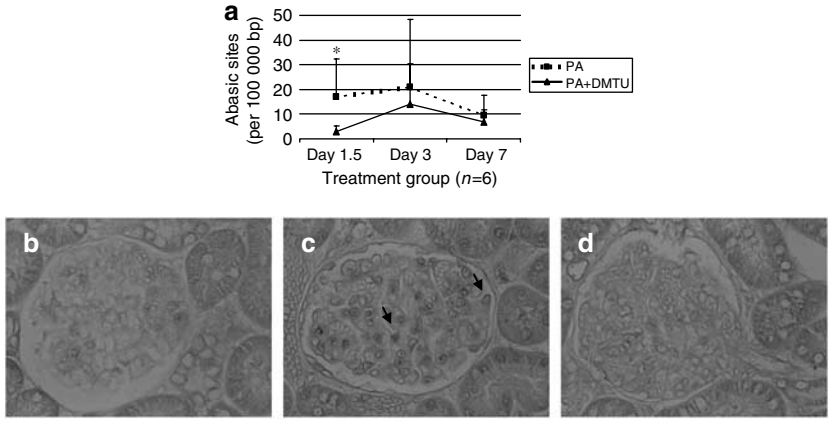

Figure 7 | DNA damage induced in PAN, attenuated by pretreatment with DMTU. (**a**) AP site assay. The number of abasic sites, as determined by the AP site assay performed on DNA harvested from isolated glomeruli, was significantly increased in rats treated with PA compared with rats receiving PA + DMTU, at day 1.5. *$P<0.05$. The difference in abasic sites was not significant at later time points. (**b**–**d**) 8-OHdG immunostaining (original magnification ×40): (**b**) Representative immunostaining for 8-OHdG in control tissues. (**c** and **d**) Representative immunostaining for 8-OHdG in tissues from (**c**) rats treated with PA alone and (**d**) rats treated with PA + DMTU, respectively (arrows indicate positive cells). In tissue from rats treated with PA alone, there was a marked increase in 8-OHdG immunostaining compared to levels in tissues from rats exposed to PA + DMTU or control conditions.

Consistent with the proteinuria data, there was a significant difference in glomerular sclerosis index among the groups (control = 2, PA = 34, PA + DMTU = 7.8) (Figure 6b). The histopathology from the PA group was typified by marked acute tubular injury with proteinaceous casts and cytoplasmic protein absorption droplets, and evidence of early segmental glomerular sclerotic lesions (Figure 6d). These results provided supporting data that PA induced glomerular and tubular injury, mediated by ROS.

DNA damage in PAN, oxidant-dependent

To determine if oxidant-dependent DNA damage was induced *in vivo*, DNA damage was measured by the AP site assay on isolated glomeruli. At the earliest time point, there was a significant difference in the number of abasic sites between the PA and PA + DMTU groups (PA = 17.13/100 000 bp, PA + DMTU = 3.06/100 000 bp; $P<0.05$) (Figure 7a). Beyond this time point, the difference between the groups diminished and was no longer significant.

To confirm the presence of DNA damage, immunostaining for 8-hydroxydeoxyguanosine (8-OHdG), an oxidized nucleotide commonly a byproduct of ROS-mediated DNA damage, was performed. In tissue from rats treated with PA (Figure 7c), there was a marked increase in 8-OHdG immunostaining compared to that in rats pretreated with DMTU (Figure 7d). Substantiating the previous findings, in addition to inducing DNA damage *in vitro*, PA also induced oxidant-mediated DNA damage *in vivo*.

Cell cycle checkpoint activation in PAN, oxidant-dependent

To determine if specific cell cycle checkpoint proteins were activated following PA-mediated oxidative DNA damage, immunostaining for checkpoint proteins in tissues harvested from experimental animals was performed. By immunohistochemistry, the number of $p21^{WAF1/CIP1}$-positive cells by day 7 was increased in the PA group compared to control and PA + DMTU groups ($p21^{WAF1/CIP1}$-positive cells per glomerulus: control 0.934, PA 4.061, PA + DMTU 2.026) (control versus PA, PA versus PA + DMTU: $P<0.05$) (Figure 8). Similarly, the number of p53-positive cells by day 7 was increased in the PA group compared to control and PA + DMTU groups (p53-positive cells per glomerulus: control 0.332, PA 5.673, PA + DMTU 2.373) (control versus PA, PA versus PA + DMTU: $P<0.05$) (Figure 9). Correlating with the *in vitro* data, cell cycle checkpoint proteins $p21^{WAF1/CIP1}$ and p53 were activated following exposure to PA. With DMTU pretreatment, the activation of these specific checkpoint proteins was reduced.

Apoptosis detection, *in vitro* and *in vivo*

Studies have shown that PA may induce podocyte apoptosis in a dose- and time-dependent manner.[20,21] Cleavage of genomic DNA during apoptosis by specific endonucleases may yield double- and single-stranded breaks.[22] To confirm that PA-induced apoptosis was not the etiology of the DNA damage detected under our experimental conditions, designed specifically to avoid apoptosis initiation by utilizing low doses and short time courses of PA, the terminal deoxynucleotidyl transferase-mediated dUTP nick end-labeling (TUNEL) assay was performed. Figure 10 shows the *in vitro* results. Following UV-C irradiation, the positive control for apoptosis induction, there were 200.75 TUNEL-positive cells per 1000. However, there was no statistically significant difference in the number of TUNEL-positive cells among the control (9.5/1000), PA (18.5/1000), and PA + DMTU (12.5/1000) groups at 6 h, the time point at which our studies showed the greatest degree of DNA damage. Figure 11 shows the *in vivo* results. TUNEL staining in tissue sections showed no statistically significant difference in the number of TUNEL-positive cells among the control (0.6/200 glomeruli),

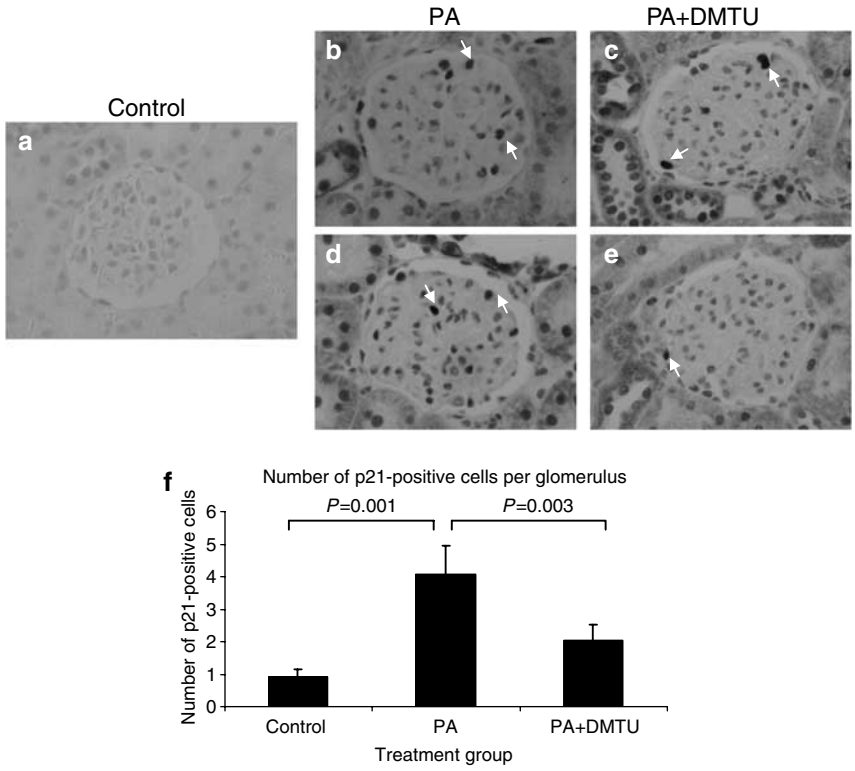

Figure 8 | Activation of cell cycle checkpoint protein p21$^{WAF1/CIP1}$ in PAN. By immunohistochemistry (original magnification $\times 40$), the number of p21$^{WAF1/CIP1}$-positive cells was increased significantly in tissues from rats treated with PA compared with time-matched animals receiving PA + DMTU (arrows indicate positive cells). (**a**) Representative immunostaining for p21$^{WAF1/CIP1}$ in control tissues. (**b** and **d**) Representative immunostaining for p21$^{WAF1/CIP1}$ in tissues treated with PA only. (**c** and **e**) Representative immunostaining for p21$^{WAF1/CIP1}$ in tissues treated with PA + DMTU. (**f**) Quantification of p21$^{WAF1/CIP1}$-positive cells per glomerulus shown in graphic form (150 glomeruli counted per section $\times 6$ animals in each group).

PA (1.8/200 glomeruli), and PA + DMTU (1.83/200 glomeruli) groups. These data support that apoptosis did not account for the DNA damage observed under our experimental design.

DISCUSSION

The highly specialized and terminally differentiated podocyte typically does not proliferate in response to injury. The detrimental decline in podocyte number post-injury leads to glomerulosclerosis.[2–6] Our group has focused on the mechanisms underlying the relative inability of podocytes to proliferate in response to most types of injury. Previously, we have shown that abnormalities in DNA synthesis, in part, underlie decreased podocyte number.[23] This is largely owing to specific cyclin-dependent kinase inhibitors.[24] A major finding in this study was that PA induced podocyte DNA damage, both *in vitro* and *in vivo*, accompanied by an increase in cell cycle checkpoint proteins p53 and p21$^{WAF1/Cip1}$. We also showed that increased ROS mediated this effect.

In PAN, the glomerular injury acutely is mediated via overproduction of ROS,[8–13] which then may interact with biomolecules including DNA, leading to potentially deleterious cellular consequences. Indirect support for the importance of ROS in the pathogenesis of PAN comes from interventional studies utilizing therapy with antioxidants, including allopurinol,[8] vitamin E,[25,26] selenium,[26] DMTU,[9,13] and grape seed extract.[27] These studies have shown beneficial effects of antioxidants, with reduction in proteinuria and improvement in glomerular morphologic changes including foot process effacement. ROS are also important mediators in the pathogenesis of glomerular injury in other experimental animal models including passive Heymann nephritis,[28] anti-Thy1 mesangial proliferative glomerulonephritis,[29] and Mpv17 gene-inactivated steroid-resistant focal segmental glomerulosclerosis.[30]

A major source of ROS in PA-induced injury is the podocyte itself, with generation of H_2O_2, $OH^{\bullet}$, superoxide anion radical, and lipid peroxidation products.[20,31] Increased ROS are associated with amplification in the activities of antioxidant enzymes including catalase, superoxide dismutase, and glutathione peroxidase.[32] PA may also induce podocyte apoptosis in a dose- and time-dependent manner, with apoptosis partially inhibited by ROS scavengers. Podocyte necrosis has been observed when high concentrations of PA are used.[20,21] Furthermore, *in vivo* studies have demonstrated increased apoptosis in the glomeruli of nephrotic animals, accompanied by increased expression of apoptosis-associated proteins.[33]

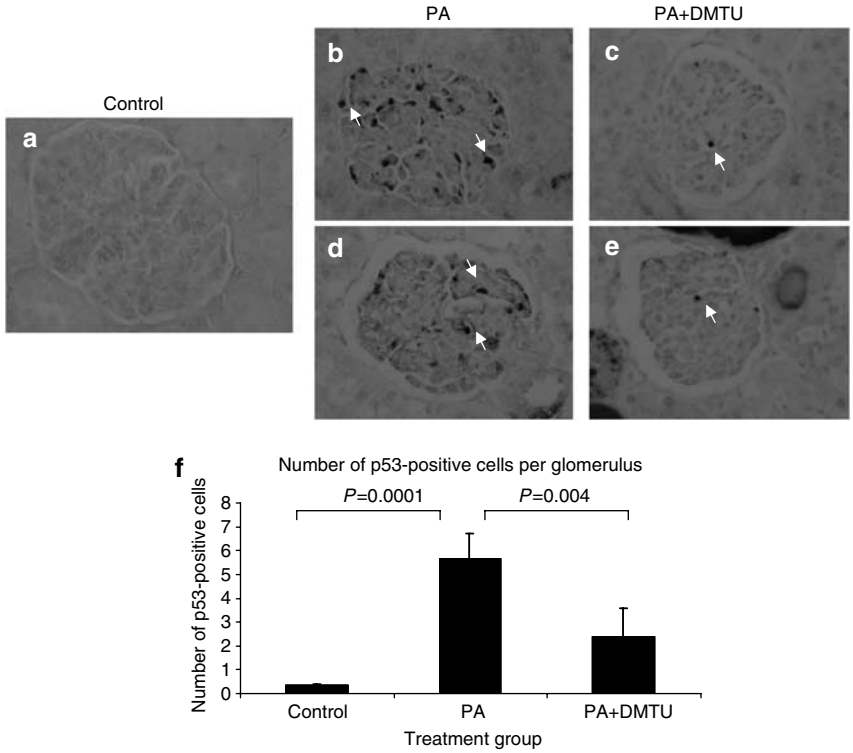

Figure 9 | Activation of cell cycle checkpoint protein p53 in PAN. By immunohistochemistry (original magnification ×40), the number of p53-positive cells was increased significantly in tissues from rats treated with PA compared with time-matched animals receiving PA + DMTU (arrows indicate positive cells). (**a**) Representative immunostaining for p53 in control tissues. (**b** and **d**) Representative immunostaining for p53 in tissues treated with PA only. (**c** and **e**) Representative immunostaining for p53 in tissues treated with PA and DMTU. **(f)** Quantification of p53-positive cells per glomerulus shown in graphic form (150 glomeruli counted per section ×6 animals in each group).

Prior studies have established that PA induces ultrastructural changes in podocytes including desquamation from the glomerular basement membrane,[34–36] cytoskeletal disaggregation,[36] damage to glomerular basement membrane charge and size barriers,[37,38] and alteration of adhesion molecule $\alpha_3\beta_1$ integrin distribution and cellular content,[39,40] all thought to be mediated, at least in part, by overproduction of ROS. The present study introduced a previously undescribed mechanism of PA-induced podocyte injury and dysfunction, namely DNA damage. In cultured podocytes, PA mediated DNA damage, measured by the DNA precipitation, AP site, and Comet assays. The attenuation of DNA damage by DMTU provided evidence that the DNA damage was mediated via ROS. PA-induced DNA damage was greatest at time point 6 h. Upregulation of DNA repair enzymes, with subsequent repair of damaged DNA, may account for the lower levels of DNA damage at later time points.

Cell cycle checkpoints are signaling pathways that make up the eukaryotic cell's response to damaged DNA and function to coordinate cell cycle progression with DNA repair, chromatin remodeling, and transcriptional programs. DNA damage-induced cell cycle arrest provides time for DNA repair or other cell fate decisions, including apoptosis or permanent exit from the cell cycle by cellular senescence.[41] In this study, PA-induced DNA damage led to activation of specific checkpoint proteins, notably p53 and p21$^{WAF1/CIP1}$, in cultured podocytes and in experimental PAN.

A possible explanation for why CHK-1 and CHK-2 expression did not substantially differ between podocytes treated with PA versus PA + DMTU is that diversity exists in the available array of checkpoint pathways between cells depending on their distinct cell cycle phase. Based on the expression, subcellular localization, and stability of specific proteins, the availability of many checkpoint components may be limited or lacking at some cell cycle stages.[41] Although CHK-1 and CHK-2 potentially could be upstream mediators of p53, p53 may also be activated by other checkpoint-transducing kinases including mutated in ataxia telangiectasia and mutated in ataxia telangiectasia and Rad3-related.

AP-endonuclease and DNA polymerase-β, two DNA repair enzymes important in the process of base excision repair, were increased in cultured podocytes following PA exposure. Activation of repair enzymes suggested that DNA damage was present and that the appropriate responses to injury were triggered in podocytes. With pre-exposure to DMTU, this activation was lessened significantly, providing further support that DNA damage was mediated by ROS.

DNA damage was significantly increased in glomeruli isolated from PA-treated animals versus the glomeruli of animals receiving PA + DMTU. The difference in the number

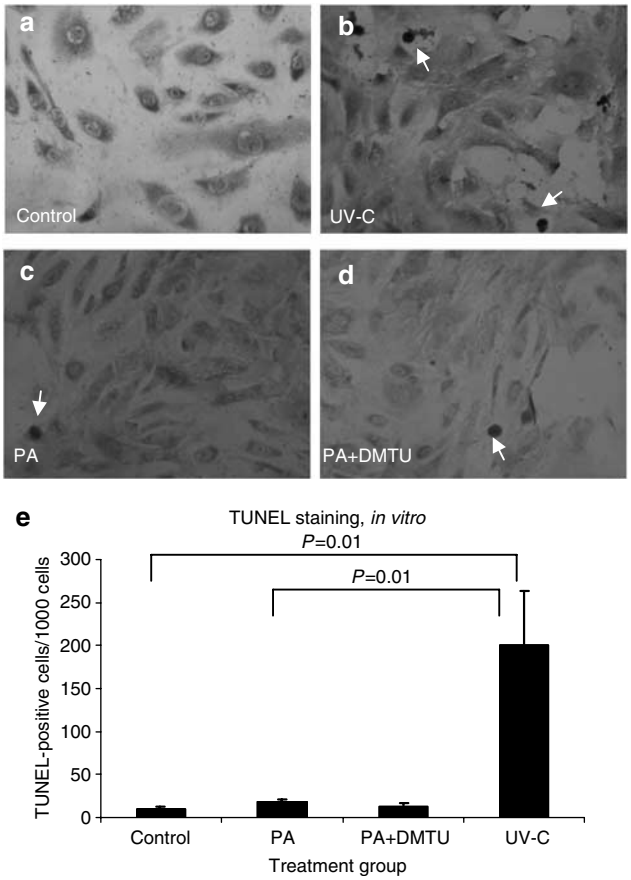

Figure 10 | Apoptosis detection following PA exposure, *in vitro*. TUNEL staining of cultured podocytes. Representative images of podocytes exposed to (**a**) negative control conditions (**b**) positive control, UV-C irradiation (**c**) PA, and (**d**) PA + DMTU. Arrows indicate TUNEL-positive cells. (original magnification × 20). (**e**) Quantification of TUNEL-positive cells per 1000 cells counted. There is no significant difference in the number of TUNEL-positive cells between negative control, PA, and PA + DMTU treatment groups (time point 6 h shown).

of abasic sites between the two groups was most notable at the earliest time point. By day 7, the level of abasic sites had declined in both groups. This decline may be attributable to repair of damaged DNA. TUNEL staining confirmed that PA-induced apoptosis was not a significant mechanism of injury under our experimental conditions.

We conclude that podocyte injury in the PAN model is, in part, mediated by the oxidizing properties of PA. In addition to the DNA damage found in the passive Heymann nephritis model of immune-mediated podocyte injury,[23] we demonstrated that DNA damage may be a more generalized response to injury. The overproduction of ROS induced podocyte DNA damage, leading to activation of checkpoint pathways to arrest or delay cell cycle progression. The resulting cell cycle arrest may be a mechanism underlying the podocyte's relative inability to proliferate following PA-induced injury. In combination with PA-induced podocyte loss from other mechanisms, including apoptosis[20,31,33] and detachment,[35] the lack of podocyte proliferation may contribute to reduced podocyte number and areas of denuded basement membrane, ultimately leading to the development of glomerulosclerosis and the progressive deterioration in kidney function.

Whether antioxidant strategies will be useful therapeutic interventions in the setting of injury induced by oxidizing podocyte toxins is unclear. There are many potential antioxidant therapies, ranging from endogenous enzymes/compounds (glutathione peroxidase-like molecules, epoetin) and trace elements (selenium) to drugs (angiotensin-converting enzyme inhibitors, β-blockers, statins, *N*-acetyl-cysteine, and metal ion chelators) and dietary antioxidants (phytoestrogens).[42] Further studies are needed to clarify the therapeutic potential of antioxidants in non-immune-mediated podocyte injury.

MATERIALS AND METHODS

Primary antibodies

Antibodies for Western blotting and immunostaining included mouse monoclonal antibodies: anti-p21$^{WAF1/CIP1}$ (BD Biosciences, San Diego, CA, USA), anti-p53 (BD Biosciences; Oncogene Research Products, San Diego, CA, USA), anti-DNA polymerase-β (Alpha Diagnostic International, San Antonio, TX, USA), anti-AP-endonuclease (Trevigen, Gaithersburg, MD, USA), anti-8-OHdG (Trevigen), anti-β-tubulin (Sigma-Aldrich, St Louis, MO, USA), anti-actin (Chemicon International, Temecula, CA, USA), and anti-glyceraldehyde-3-phosphate dehydrogenase (Abcam, Cambridge, MA, USA).

Mouse podocytes in culture

A conditionally immortalized mouse podocyte cell line isolated from H-2K^b-tsA58 transgenic mice kidneys (Jackson Laboratory, Bar Harbor, ME, USA) was used *in vitro*.[43–45] In this cell line, γ-interferon-inducible H-2K^b promoter controls a temperature-sensitive SV40 large T-cell antigen. To induce proliferation, cells were grown on Primaria plates (VWR International, West Chester, PA, USA) coated with collagen I (BD Biosciences) at 33°C in Rosewell Park Memorial Institute 1640 media (Invitrogen, Grand Island, NY, USA) supplemented with 10% fetal calf serum (Hyclone, Logan, UT, USA), with added recombinant mouse γ-interferon 50 U/ml (Roche, Indianapolis, IN, USA).[46] To induce the quiescent, differentiated phenotype, cells were grown at 37°C without γ-interferon (growth-restrictive condition). Experiments were performed at least three times, on growth-restricted days 12–14, utilizing more than one cell clone to verify reproducibility of results. The cell lines were derived in our lab, identified and characterized by immunostaining and reverse transcription-polymerase chain reaction, as described previously.[47]

DNA damage detection *in vitro* following exposure to PA

Following preliminary dose-defining studies, the DNA precipitation assay[48] was used to detect PA-induced DNA damage. After incubation with 0.5 μCi/ml ^{3}H-thymidine to allow for DNA incorporation, podocytes were exposed to PA 30 μg/ml for 2 h. Cells were washed with Hank's Balanced Salt Solution (Irvine Scientific, Santa Ana, CA, USA) and incubated in medium until a series of time points. At time of harvest, podocytes were lysed, incubated with 12 M KCl at 65°C for 10 min, iced for 5 min, and

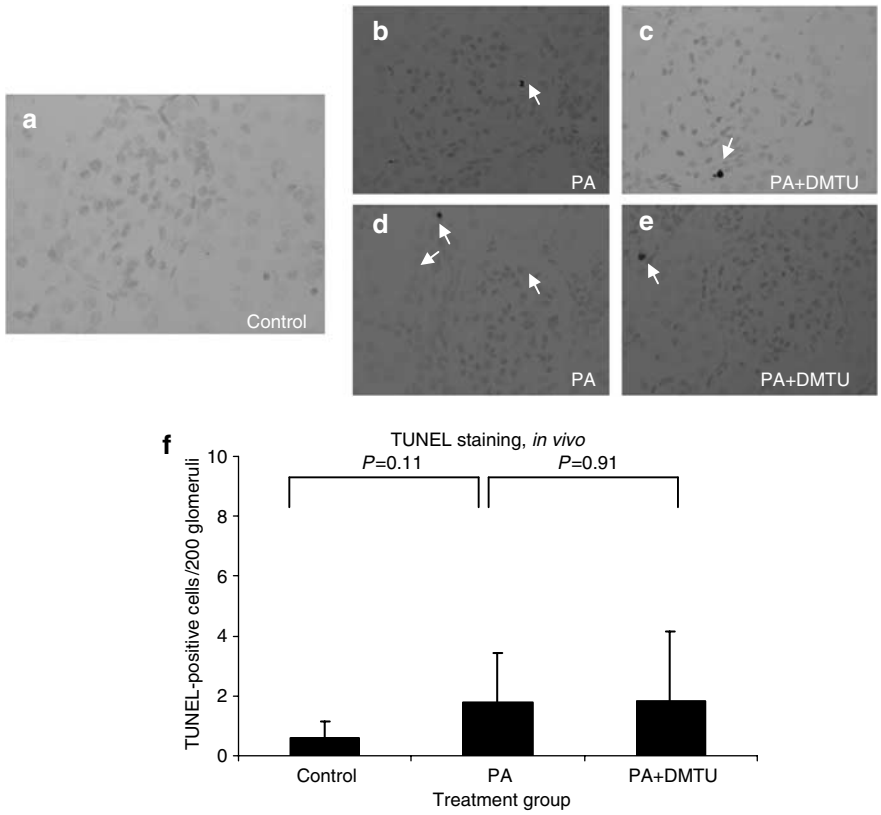

Figure 11 | Apoptosis detection following PA exposure, *in vivo*. TUNEL staining of tissue sections. Representative images of tissue sections from rats in (**a**) control group versus (**b** and **d**) groups treated with PA alone or (**c** and **e**) PA + DMTU. (**d** and **e**) TUNEL-positive cells in the tubulointerstitium adjacent to glomeruli without positive cells. (**f**) Quantification of TUNEL-positive cells per 200 glomeruli counted. There is no significant difference in the number of TUNEL-positive cells between control, PA, and PA + DMTU treatment groups.

centrifuged (3200 *g*) to separate precipitated chromatin DNA from damaged DNA (supernatant). Supernatants and DNA pellets were dissolved separately in scintillation fluid and counted in a Beckman 3500 scintillation counter. The percentage of ssDNA was calculated.

ROS commonly induce depurination and depyrimidination.[7] Therefore, the AP site assay was the second detection method of PA-induced DNA damage, using the DNA damage quantification kit (Dojindo Molecular Technologies, Gaithersburg, MD, USA). Briefly, DNA was isolated from podocytes using the DNeasy isolation kit (Qiagen, Valencia, CA, USA). AP sites were detected using an aldehyde-reactive probe reagent. AP sites were tagged with biotin, and the DNA was bound to a microtiter plate along with aldehyde-reactive probe-tagged DNA standards. The sites were visualized using peroxidase streptavidin. The number of AP sites in the sample DNA was determined by comparing absorbance at 650 nm to the standard curve.

To confirm PA-induced DNA damage, the single-cell gel electrophoresis assay (Comet assay) (Trevigen), was utilized.[49–51] Briefly, podocytes were gently harvested and embedded in an agarose layer on a microscope slide. Cells were lysed to remove cellular proteins and DNA was uncoiled under alkaline conditions. After unwinding, DNA was electrophoresed for 20 min under alkaline conditions and stained with fluorescent dye. In contrast to undamaged and supercoiled DNA that remains within the nuclear cell membrane, the podocytes with damaged DNA, which migrated away from the nucleus, demonstrated the characteristic long 'comet tail'. The extent of DNA liberated from the head of the 'comet' was directly proportional to DNA damage.

DNA damage detection *in vitro* following exposure to PA ± DMTU

Studies have highlighted the importance of hydroxyl radical ($OH^{\bullet}$) in ROS-mediated injury during the induction phase of PAN.[10] Highly reactive and toxic, $OH^{\bullet}$ can generate modifications in DNA including sugar/base alterations, strand breaks, and DNA–protein cross-links.[15,16,43] To determine the role of oxidants in PA-induced DNA damage, podocytes were pretreated with the $OH^{\bullet}$ scavenger DMTU (Sigma-Aldrich).

One hour before PA exposure, podocytes were incubated in medium with DMTU 10 mM. One-hour incubation with 2.5 mM H_2O_2 served as the positive control for oxidant-induced DNA damage. Although H_2O_2 itself is considered relatively non-reactive toward DNA, much of the H_2O_2-mediated DNA damage is secondary to $OH^{\bullet}$ generation via the Fenton reaction.[7]

Western blot analysis

Because activated checkpoints induce cell cycle arrest following exposure to DNA-damaging agents,[7] Western blotting was performed to measure the expression of specific cell cycle checkpoint proteins in podocytes exposed to PA ± DMTU.[52] Cells were harvested by trypsin digestion and pelleted by centrifugation (1200 r.p.m. for 5 min). Protein was extracted using TG buffer,[46] in the presence of a protease inhibitor cocktail (Roche) and phosphatase inhibitors sodium orthovanadate and sodium fluoride (Sigma-Aldrich). Following a freeze–thaw cycle, lysates were cleared by centrifugation (16 000 r.p.m. for 10 min), and protein concentrations were determined by the bicinchoninic acid

protein assay (Pierce, Rockford, IL, USA). Protein extracts of 5–15 μg were separated under reduced conditions on 12–15% sodium dodecyl sulfate-polyacrylamide gels and transferred to polyvinyl difluoride membranes (PerkinElmer, Boston, MA, USA).[24,53,54] Membranes were incubated with antibodies to $p21^{WAF1/CIP1}$, p53, growth arrest, DNA damage-inducible-45α, AP-endonuclease, DNA polymerase-β, CHK-1, and CHK-2. To ensure equal protein loading, antibodies to housekeeping proteins tubulin, actin, and glyceraldehyde-3-phosphate dehydrogenase were used. Bands were detected with chromagen 5-bromo-4-chloro-3-inodyl phosphate/nitro blue tetrazolium (Sigma-Aldrich). Densitometry was performed with the NIH image analysis program ImageJ. Three separate experiments were performed for each Western blot analysis and the densitometry results were averaged, with normalization for differences in protein loading.

PAN model

To test the hypothesis that PA induced podocyte DNA damage *in vivo*, the PAN model[55] was induced in male Sprague–Dawley rats (Charles River Laboratories, Wilmington, MA, USA). After preliminary studies to define the optimal dose to achieve mild-to-moderate disease, identifying a dose that would cause DNA damage without significant accompanying apoptosis or necrosis, rats aged 60 days, weighing 200–300 g, were divided into treatment groups ($n = 6$/group/time point): PA, PA + DMTU, and control, killed at days 1.5, 3, and 7.[8,9,56,57] The PA groups received a single injection of PA dissolved in 0.9% NaCl, at 6 mg/100 g body weight via tail vein. The PA + DMTU groups received DMTU dissolved in 0.9% NaCl, 500 mg/kg intraperitoneally one hour before PA injection, then 125 mg/kg intraperitoneally twice a day until killing. The control animals were injected with equal volume of 0.9% NaCl substituted for both PA and DMTU. Each animal was anesthetized with 100% ethyl ether (VWR) in an inhalation chamber before tail vein injections. Animals were anesthetized in an isoflurane (Halocarbon Labs, North Augusta, SC, USA) and oxygen vaporizer chamber before intraperitoneal injections. Before killing, urine collections were obtained in metabolic cages to determine 24-h protein and creatinine excretion. Urine protein was measured by the sulfosalicylic acid method (standards from Dade Diagnostics, Brisbane, Australia).[58] Urine creatinine levels were determined via a colorimetric microplate assay (Oxford Biomedical, Oxford, MI, USA). Death was induced by exsanguination following anesthetization with 100% ethyl ether. Blood samples, obtained at time of killing via vena caval puncture, were centrifuged (12 000 *g* for 5 min) and plasma was collected for measurement of blood urea nitrogen (Sigma-Aldrich). Tissues were obtained for renal biopsies and glomerular isolation. All animal procedures were conducted in accord with the Institutional Animal Care and Use Committee.

Isolation of glomeruli

Preparation of isolated glomeruli was performed at 4°C, with kidney tissue from one rat used per preparation.[52] After discarding medulla and papilla, finely minced cortices were passed through three differential sieves (200, 140, and 80 μm) using 2000 ml of normal saline. Glomeruli were washed and resuspended in 50 ml of saline. Quantitation of glomeruli was performed in aliquots of glomerular suspension by phase microscopy, with purity >95% for all preparations. Following centrifugation (1000 r.p.m. at 4°C for 10 min), supernatant was decanted, and DNA isolation and purification was performed from the pelleted glomeruli.

Measuring DNA damage *in vivo*

DNA was isolated and purified from glomerular isolates via the DNeasy tissue kit. DNA damage was detected by counting abasic sites using the DNA damage quantification kit.

Immunohistochemistry

Indirect immunoperoxidase immunostaining was performed on formalin-fixed paraffin-embedded kidney specimens.[53] Briefly, 4-μm tissue sections were deparaffinized in Histo-Clear (National Diagnostics, Atlanta, GA, USA) and rehydrated in graded ethanol. Endogenous peroxidases were blocked with 3% H_2O_2, followed by overnight incubation with primary antibody diluted in 1% bovine serum albumin in phosphate-buffered saline (PBS). After washing in PBS, sections were incubated with biotinylated secondary antibody, diluted in 1% bovine serum albumin in PBS, for 1 h at room temperature. ABC (Avidin and Biotinylated horseradish peroxidase macromolecular Complex)-Elite reagent (Vector Laboratories, Burlingame, CA, USA) was used for signal amplification and 3,3′-diaminobenzidine (Sigma-Aldrich) catalyzed by $NiCl_2$ was used as chromagen. Slides were counterstained with methyl green, dehydrated, and coverslipped.

Immunostaining for 8-OHdG, was performed on methacarn-fixed tissue.[59] Briefly, following deparaffinization and rehydration, slides were pretreated with proteinase K (Roche) and RNase (Qiagen). DNA was denatured with 4 N HCl, followed by Tris-buffered saline neutralization. 10% fetal calf serum in 10 mM Tris-HCl was used to block unspecific sites. Sections were incubated overnight at 4°C with primary antibody diluted in 10 mM Tris-HCl, 10% fetal calf serum . After washing with PBS, sections were incubated with the secondary antibody at 37°C for 30 min. ABC-Elite reagent was used for signal amplification. 3,3′-diaminobenzidine with 30% H_2O_2 was used as chromagen. Slides were counterstained with hematoxylin, dehydrated, and coverslipped.

Apoptosis detection

TUNEL staining was utilized to exclude the possibility of significant apoptosis under our experimental conditions. The protocol was a modification of methods described previously.[60] Briefly, cultured podocytes were fixed with 10% buffered formalin overnight at 4°C. Following rehydration with PBS, endogenous peroxidases were inactivated with 3% H_2O_2. Cells were treated with citric acid to enhance antigen retrieval. Nuclei were permeabilized by incubation with proteinase K for 20 min at room temperature. Following incubation in One-Phor-All buffer (GE Healthcare, Piscataway, NJ, USA), fragmented DNA was labeled by exposure of cells to diluted terminal deoxynucleotidyl transferase (GE Healthcare) and biotin-14-dATP (Invitrogen) for 60 min. The reaction was terminated with PBS. ABC-Elite reagent was used for signal amplification. 3,3′-diaminobenzidine with $NiCl_2$ was used as chromagen. Cells were counterstained with Camco Quik stain (Cambridge Diagnostic, Fort Lauderdale, FL, USA).

Similarly, *in vivo*, TUNEL staining was performed on 4-μm formalin-fixed paraffin-embedded tissue sections. Following deparaffinization and rehydration, the above protocol was followed. Slides were counterstained with methyl green, dehydrated, and coverslipped.

Statistical analysis

For comparison of mean values between two groups, the unpaired *t* test was used. All values are means ± s.d. except where otherwise

indicated. The experimental findings were considered statistically significant if $P<0.05$. All photomicrographs were made at similar intensity and background. During data analysis, the observer was blinded to the treatment categories.

ACKNOWLEDGMENTS

This work was supported by National Institutes of Health grants to SJS (DK60525, DK56799, and DK 51096), by National Institutes of Health grant to CBM (3 RO1 DK051096-06S1), and by the American Diabetes Association. SJS is also an Established Investigator of the American Heart Association.

REFERENCES

1. Pavenstadt H, Kriz W, Kretzler M. Cell biology of the glomerular podocyte. *Physiol Rev* 2003; **83**: 253–307.
2. Kriz W, Gretz N, Lemley KV. Progression of glomerular diseases: is the podocyte the culprit? *Kidney Int* 1998; **54**: 687–697.
3. Kim YH, Goyal M, Kurnit D *et al.* Podocyte depletion and glomerulosclerosis have a direct relationship in the PAN-treated rat. *Kidney Int* 2001; **60**: 957–968.
4. Pagtalunan ME, Miller PL, Jumping-Eagle S *et al.* Podocyte loss and progressive glomerular injury in type II diabetes. *J Clin Invest* 1997; **99**: 342–348.
5. Wharram BL, Goyal M, Wiggins JE *et al.* Podocyte depletion causes glomerulosclerosis: diphtheria toxin-induced podocyte depletion in rats expressing human diphtheria toxin receptor transgene. *J Am Soc Nephrol* 2005; **16**: 2941–2952.
6. Ichikawa I, Ma J, Motojima M, Matsusaka T. Podocyte damage damages podocytes: autonomous vicious cycle that drives local spread of glomerular sclerosis. *Curr Opin Nephrol Hypertens* 2005; **14**: 205–210.
7. Shackelford RE, Kaufmann WK, Paules RS. Oxidative stress and cell cycle checkpoint function. *Free Radic Biol Med* 2000; **28**: 1387–1404.
8. Diamond JR, Bonventre JV, Karnovsky MJ. A role for oxygen free radicals in aminonucleoside nephrosis. *Kidney Int* 1986; **29**: 478–483.
9. Thakur V, Walker PD, Shah SV. Evidence suggesting a role for hydroxyl radical in puromycin aminonucleoside-induced proteinuria. *Kidney Int* 1988; **34**: 494–499.
10. Gwinner W, Landmesser U, Brandes RP *et al.* Reactive oxygen species and antioxidant defense in puromycin aminonucleoside glomerulopathy. *J Am Soc Nephrol* 1997; **8**: 1722–1731.
11. Beaman M, Birtwistle R, Howie AJ *et al.* The role of superoxide anion and hydrogen peroxide in glomerular injury induced by puromycin aminonucleoside in rats. *Clin Sci (London)* 1987; **73**: 329–332.
12. Shibouta Y, Terashita Z, Imura Y *et al.* Involvement of thromboxane A2, leukotrienes and free radicals in puromycin nephrosis in rats. *Kidney Int* 1991; **39**: 920–929.
13. Ricardo SD, Bertram JF, Ryan GB. Antioxidants protect podocyte foot processes in puromycin aminonucleoside-treated rats. *J Am Soc Nephrol* 1994; **4**: 1974–1986.
14. Nakamura K, Kojima K, Arai T *et al.* Dipyridamole and dilazep suppress oxygen radicals in puromycin aminonucleoside nephrosis rats. *Eur J Clin Invest* 1998; **28**: 877–883.
15. Cooke MS, Evans MD, Dizdaroglu M, Lunec J. Oxidative DNA damage: mechanisms, mutation, and disease. *FASEB J* 2003; **17**: 1195–1214.
16. Halliwell B, Gutteridge JMC. *Free radicals in biology and medicine*, 3rd edn. Oxford University Press: Oxford New York, Clarendon Press, 2003.
17. Raij L, Azar S, Keane W. Mesangial immune injury, hypertension, and progressive glomerular damage in Dahl rats. *Kidney Int* 1984; **26**: 137–143.
18. Saito T, Sumithran E, Glasgow EF, Atkins RC. The enhancement of aminonucleoside nephrosis by the co-administration of protamine. *Kidney Int* 1987; **32**: 691–699.
19. Nakamura T, Obata J, Kimura H *et al.* Blocking angiotensin II ameliorates proteinuria and glomerular lesions in progressive mesangioproliferative glomerulonephritis. *Kidney Int* 1999; **55**: 877–889.
20. Sanwal V, Pandya M, Bhaskaran M *et al.* Puromycin aminonucleoside induces glomerular epithelial cell apoptosis. *Exp Mol Pathol* 2001; **70**: 54–64.
21. Fernandez L, Romero M, Soto H, Mosquera J. Increased apoptosis in acute puromycin aminonucleoside nephrosis. *Exp Nephrol* 2001; **9**: 99–108.
22. Hengartner MO. The biochemistry of apoptosis. *Nature* 2000; **407**: 770–776.
23. Pippin JW, Durvasula R, Petermann A *et al.* DNA damage is a novel response to sublytic complement C5b-9-induced injury in podocytes. *J Clin Invest* 2003; **111**: 877–885.
24. Shankland SJ, Floege J, Thomas SE *et al.* Cyclin kinase inhibitors are increased during experimental membranous nephropathy: potential role in limiting glomerular epithelial cell proliferation *in vivo*. *Kidney Int* 1997; **52**: 404–413.
25. Trachtman H, Schwob N, Maesaka J, Valderrama E. Dietary vitamin E supplementation ameliorates renal injury in chronic puromycin aminonucleoside nephropathy. *J Am Soc Nephrol* 1995; **5**: 1811–1819.
26. Pedraza-Chaverri J, Arevalo AE, Hernandez-Pando R, Larriva-Sahd J. Effect of dietary antioxidants on puromycin aminonucleoside nephrotic syndrome. *Int J Biochem Cell Biol* 1995; **27**: 683–691.
27. Mattoo TK, Kovacevic L. Effect of grape seed extract on puromycin-aminonucleoside-induced nephrosis in rats. *Pediatr Nephrol* 2003; **18**: 872–877.
28. Neale TJ, Ojha PP, Exner M *et al.* Proteinuria in passive Heymann nephritis is associated with lipid peroxidation and formation of adducts on type IV collagen. *J Clin Invest* 1994; **94**: 1577–1584.
29. Budisavljevic MN, Hodge L, Barber K *et al.* Oxidative stress in the pathogenesis of experimental mesangial proliferative glomerulonephritis. *Am J Physiol Renal Physiol* 2003; **285**: F1138–F1148.
30. Binder CJ, Weiher H, Exner M, Kerjaschki D. Glomerular overproduction of oxygen radicals in Mpv17 gene-inactivated mice causes podocyte foot process flattening and proteinuria: a model of steroid-resistant nephrosis sensitive to radical scavenger therapy. *Am J Pathol* 1999; **154**: 1067–1075.
31. Kawaguchi M, Yamada M, Wada H, Okigaki T. Roles of active oxygen species in glomerular epithelial cell injury *in vitro* caused by puromycin aminonucleoside. *Toxicology* 1992; **72**: 329–340.
32. Vega-Warner V, Ransom RF, Vincent AM *et al.* Induction of antioxidant enzymes in murine podocytes precedes injury by puromycin aminonucleoside. *Kidney Int* 2004; **66**: 1881–1889.
33. Rincon J, Romero M, Viera N *et al.* Increased oxidative stress and apoptosis in acute puromycin aminonucleoside nephrosis. *Int J Exp Pathol* 2004; **85**: 25–33.
34. Ricardo SD, Bertram JF, Ryan GB. Reactive oxygen species in puromycin aminonucleoside nephrosis: *in vitro* studies. *Kidney Int* 1994; **45**: 1057–1069.
35. Ryan GB, Karnovsky MJ. An ultrastructural study of the mechanisms of proteinuria in aminonucleoside nephrosis. *Kidney Int* 1975; **8**: 219–232.
36. Whiteside CI, Cameron R, Munk S, Levy J. Podocytic cytoskeletal disaggregation and basement-membrane detachment in puromycin aminonucleoside nephrosis. *Am J Pathol* 1993; **142**: 1641–1653.
37. Olson JL, Rennke HG, Venkatachalam MA. Alterations in the charge and size selectivity barrier of the glomerular filter in aminonucleoside nephrosis in rats. *Lab Invest* 1981; **44**: 271–279.
38. Garin EH, Shirey AJ. Glomerular basement membrane heparan sulfate glycosaminoglycan in aminonucleoside of puromycin nephrosis. *Child Nephrol Urol* 1988; **9**: 121–126.
39. Kojima K, Matsui K, Nagase M. Protection of alpha(3) integrin-mediated podocyte shape by superoxide dismutase in the puromycin aminonucleoside nephrosis rat. *Am J Kidney Dis* 2000; **35**: 1175–1185.
40. Krishnamurti U, Zhou B, Fan WW *et al.* Puromycin aminonucleoside suppresses integrin expression in cultured glomerular epithelial cells. *J Am Soc Nephrol* 2001; **12**: 758–766.
41. Lukas J, Lukas C, Bartek J. Mammalian cell cycle checkpoints: signalling pathways and their organization in space and time. *DNA Repair (Amsterdam)* 2004; **3**: 997–1007.
42. Tylicki L, Rutkowski B, Horl WH. Antioxidants: a possible role in kidney protection. *Kidney Blood Press Res* 2003; **26**: 303–314.
43. Jat PS, Noble MD, Ataliotis P *et al.* Direct derivation of conditionally immortal cell lines from an H-2Kb-tsA58 transgenic mouse. *Proc Natl Acad Sci USA* 1991; **88**: 5096–5100.
44. Mundel P, Reiser J, Zuniga Mejia Borja A *et al.* Rearrangements of the cytoskeleton and cell contacts induce process formation during differentiation of conditionally immortalized mouse podocyte cell lines. *Exp Cell Res* 1997; **236**: 248–258.
45. Mundel P, Reiser J, Kriz W. Induction of differentiation in cultured rat and human podocytes. *J Am Soc Nephrol* 1997; **8**: 697–705.
46. Griffin SV, Hiromura K, Pippin J *et al.* Cyclin-dependent kinase 5 is a regulator of podocyte differentiation, proliferation, and morphology. *Am J Pathol* 2004; **165**: 1175–1185.
47. Wada T, Pippin JW, Terada Y, Shankland SJ. The cyclin-dependent kinase inhibitor p21 is required for TGF-beta1-induced podocyte apoptosis. *Kidney Int* 2005; **68**: 1618–1629.

48. Leanderson P, Wennerberg K, Tagesson C. DNA microfiltration assay: a simple technique for detecting DNA damage in mammalian cells. *Carcinogenesis* 1994; **15**: 137–139.
49. Cook PR, Brazell IA. Detection and repair of single-strand breaks in nuclear DNA. *Nature* 1976; **263**: 679–682.
50. Ostling O, Johanson KJ. Microelectrophoretic study of radiation-induced DNA damages in individual mammalian cells. *Biochem Biophys Res Commun* 1984; **123**: 291–298.
51. Singh NP, McCoy MT, Tice RR, Schneider EL. A simple technique for quantitation of low levels of DNA damage in individual cells. *Exp Cell Res* 1988; **175**: 184–191.
52. Shankland SJ, Hugo C, Coats SR *et al.* Changes in cell-cycle protein expression during experimental mesangial proliferative glomerulonephritis. *Kidney Int* 1996; **50**: 1230–1239.
53. Hiromura K, Haseley LA, Zhang P *et al.* Podocyte expression of the CDK-inhibitor p57 during development and disease. *Kidney Int* 2001; **60**: 2235–2246.
54. Shankland SJ, Pippin J, Flanagan M *et al.* Mesangial cell proliferation mediated by PDGF and bFGF is determined by levels of the cyclin kinase inhibitor p27Kip1. *Kidney Int* 1997; **51**: 1088–1099.
55. Lannigan R, Kark R, Pollak VE. The effect of a single intravenous injection of aminonucleoside of puromycin on the rat kidney: a light- and electron-microscope study. *J Pathol Bacteriol* 1962; **83**: 357–362.
56. Tsuruya K, Tokumoto M, Ninomiya T *et al.* Antioxidant ameliorates cisplatin-induced renal tubular cell death through inhibition of death receptor-mediated pathways. *Am J Physiol Renal Physiol* 2003; **285**: F208–218.
57. Walker PD, Shah SV. Evidence suggesting a role for hydroxyl radical in gentamicin-induced acute renal failure in rats. *J Clin Invest* 1988; **81**: 334–341.
58. Shankland SJ, Pippin J, Pichler RH *et al.* Differential expression of transforming growth factor-beta isoforms and receptors in experimental membranous nephropathy. *Kidney Int* 1996; **50**: 116–124.
59. Yarborough A, Zhang YJ, Hsu TM, Santella RM. Immunoperoxidase detection of 8-hydroxydeoxyguanosine in aflatoxin B1-treated rat liver and human oral mucosal cells. *Cancer Res* 1996; **56**: 683–688.
60. Gavrieli Y, Sherman Y, Ben-Sasson SA. Identification of programmed cell death *in situ* via specific labeling of nuclear DNA fragmentation. *J Cell Biol* 1992; **119**: 493–501.